International Journal of Applied Pharmaceutics

ISSN- 0975-7058 Vol 15, Issue 6, 2023

Original Article

DESIGN AND OPTIMIZATION OF NANO ENCAPSULATED *BERBERIS ASIATICA* BIO COMPOUNDS

BHARGAVI POSINASETTY[1], SRIVIDYA KOMMINENI[2], RAJASEKHAR KOMARLA KUMARACHARI[3], KISHORE BANDARAPALLE*

[1]Prometrika LLC, Cambridge, MA-02140, USA. Government Dental College and Research Institute, Bellary, Karnataka, India. [2]Upsher-Smith laboratories, Minnesota-55369, USA. Sri Padmavathi School of Pharmacy, Tiruchanur, Tirupati-517503, Andhra Pradesh. [3]Department of Pharmaceutical Chemistry, Sri Padmavathi School of Pharmacy, Tiruchanur, Tirupati-517503, Andhra Pradesh, India. *Department of Pharmaceutics, Sri Padmavathi School of Pharmacy, Tiruchanur, Tirupati-517503, Andhra Pradesh, India

[*]Corresponding author: Kishore Bandarapalle; Email: kishore.brr89@gmail.com

Received: 08 Jul 2023, Revised and Accepted: 14 Aug 2023

ABSTRACT

Objective: The current study goal is to develop and optimize nanoencapsulated biocompounds of *Berberis asiatica* (BCBA) utilizing the ionic gelation process to target the kidney for antiurolithiatic activity.

Methods: Nanoencapsulated BCBA was prepared employing the ionic gelation method. Box Behnken Design (BBD) 3-factor, 3-level is used to examine the effects of formulation parameters and to enhance the desired responses. Characterization studies include Fourier transform infrared (FTIR), X-ray diffraction (XRD), particle size, zeta potential, scanning electron microscopy (SEM), and transmission electron microscopy (TEM) performed to study the quality of optimized nanoparticles.

Results: Mathematical equations and response surface plots were used to relate the dependent and independent variables. Diagnostic charts were used to show the varied factor level permutations. The percentages of entrapment efficiency (% EE) and drug release (% DR) used in evaluation studies of optimized biocompounds of *Berberis asiatica* nanoparticles (OBCBANPs) were determined to be 83.7% and 78.33%, respectively. The Fourier transform infrared (FTIR) results showed that chitosan, sodium tripolyphosphate (NaTPP), and BACB were compatible. Due to chitosan and NaTPP gelation in the case of OBCBANPs, X-ray diffraction (XRD) analyses have acknowledged the crystalinity. The particle size and zeta potential of the optimized formulation, found to be 95.4 nm and 31 mV, respectively, indicate the nanoparticles are in the nano range and possess extreme stability by preventing particle convergence. Scanning Electron Microscopy (SEM) and Transmission Electron Microscopy (TEM) studies reveal that the optimized formulation nanoparticles are spherical in shape, homogeneous, and have little aggregation. The accelerated stability studies showed that the optimized formulation was stable at different temperatures and relative humidity.

Conclusion: The stable optimized formulation was prepared, evaluated, and characterized. BBD is employed to optimize the formulation by minimizing the number of experimental runs and enhancing the desired responses. The optimized formulation further needs to investigate the *invivo* studies for antiurolithiatic activity by targeting the kidney.

Keywords: *Berberis asiatica*, Nanoparticles, Box-behnken design, Chitosan, Entrapment efficiency

DOI: https://dx.doi.org/10.22159/ijap.2023v15i6.48800. Journal homepage: https://innovareacademics.in/journals/index.php/ijap

INTRODUCTION

One of the well-known technologies is nanotechnology, which carries out a wide variety of tasks, among which improving bioavailability and directing medication toward particular organs are well-proven and suggested. In the present research, a chitosan nanoparticle was designed to encapsulate a preselected plant extract that included bioactive chemicals. Due to its distinctive qualities, such as being biocompatible and biodegradable, low molecular weight chitosan was widely exploited, particularly in the creation of polymeric nanoparticles, particularly in the present research into the therapy of renal calculi production [1, 2].

Bioactive components from *Berberis asiatica* used in the study because they have antioxidant, diuretic, alkalinizing, and hypocalciuric qualities, all of which are crucial for treating urolithiasis disease [3, 4]. In renal tubular epithelial cells, aminoglycoside has been found to be a well-known ligand of megalin receptors. It has been astonishingly observed that aminoglycosides and chitosan polymers have a similar glucosamine structure. Then, chitosan was discovered to be an effective ligand for megalin receptors on renal tubular epithelial cells in previous research, increasing drug accumulation in the region of interest.

Chitosan frequently performs an important role, i.e., directing bioactive substances to renal cells, which improves the management of renal calculi, in addition to its biocompatible and biodegradable qualities. In order to increase medication targeting and bioavailability in the treatment of renal calculi in contrast to bioactive compounds administered alone, the current study concentrated on the production of chitosan nanoparticles loaded with bioactive components of selected plant extracts [5-11].

The design of experiments (DOE) has been used to effectively guide the selection of experiments to be carried out in an optimal way, as well as to minimize process variation. Optimizing the formulation by minimizing the number of experimental runs and time investment is the main goal of employing DOE. The Response Surface Methodology (RSM), one of the several design strategies, is a computational technique created using empiric models for the data acquired from experiments conducted. In actual practice, the Box Behnken Design (BBD), RSM approach is frequently used to assess and optimize the main, interactive, and quadratic impacts of the independent variables on dependent variables. Each independent variable must have three levels in the design. The impact of various factors may be examined on data using analysis of variance (ANOVA) and linear regression studies. Therefore, the present study is focused on the optimization of nanoencapsulated biocompounds of Berberis asiatica by BBD, RSM and targeting the kidney for their antiurolithiatic activity. The aforementioned background has caused current research to concentrate on the targeting of bioactive compound-loaded chitosan nanoparticles.

MATERIALS AND METHODS

Chemicals

The study made use of analytical grade chemicals (Sigma Aldrich, Hi-media, and Merck India Ltd).

Collection and preparation of an aqueous extract of *Berberis asiatica* (BCBA)

The B. asiatica heartwood was obtained from the Sri Srinivasa ayurvedic pharmacy in Tirupati. Dr. K. Madhava chetty, Assistant Professor, Department of Botany, Sri Venkateswara University, Tirupati, identified and authenticated it(voucher No: 0663). The heartwood had been dried and roughly ground. At room temperature, 200 g of heartwood powder was macerated with 1liter of distilled water for 24 h. The extract was concentrated, and the resulting semisolid mass of 20 g was housed in an airtight container devoid of excess heat, moisture, and air and labelled BCBA.

UV spectral analysis of BCBA

The calibration curve is the primary basis for estimating drug entrapment efficiency in nanoparticles and *in vitro* drug release. To determine the maximum absorption wavelength of selected candidates, UV spectral analysis of BCBA was undertaken using a UV-Visible spectrophotometer between 200 and 400 nm.

Preparation of biocompounds of *Berberis asiatica* loaded nanoparticles (BCBANPs)

Using the ionic gelation process, BCBANPs were made by entrapping BCBA in chitosan nanoparticles.

Box behnken design (BBD)

The method was used to explore the main, interaction, and quadratic impacts of the variables on the formulation's efficacy and subsequent optimization. A non-linear quadratic model was developed using Design Expert software version 11. Variables are classified into two types: independent variables, also known as factors, and dependent variables, also known as responses. The quantities of chitosan, sodium tripolyphosphate (NaTPP), and BCBA are the independent variables in this study. The dependent variables are percent entrapment efficiency and percent drug release (table 1). A, B, and C are the factors for chitosan, sodium tripolyphosphate, and BCBA, respectively, while R1 and R2 are the factors for percent entrapment efficacy and percent drug release, respectively [12, 13].

Table 1: Independent and dependent variables

Independent variables (Factors)	Dependent variables (Responses)
Polymer (Chitosan)	Percent entrapment efficiency
Cross-linking agent (NaTPP)	
Drug (BCBA)	Percent drug release

The polynomial equation generated by Box-Behnken Design was followed as.

$$Y=\beta0+\beta1A+\beta2B+\beta3C+\beta4AB+\beta5AC+\beta6BC+\beta7A2+\beta8B2+\beta9C2+E$$

Where, Y = analyzed response,

β0 = intercept,

β1 to β9 are the regression coefficients,

A, B and C = independent variables (factors), (chitosan, NaTPP and BCBA),

E is error term.

The main goal of surface response graphs and two-dimensional outlines, which were based on the polynomial or model equation, was to investigate the relationship between responses, mixture components, and numeric variables.

Additionally, the research included a model adequacy evaluation using residual versus predicted runs, predicted versus actual values, a normal residual plot, residual versus actual runs, and residual versus run plots.

Evaluation of nanoparticles

Entrapment efficiency

By quantifying the percentage of free drug in the supernatant collected as a result of centrifugation, one can determine the quantity of drug trapped in chitosan nanoparticles. After the stirring and sonication process was finished, the preparation was shifted to the centrifuge tube and positioned in a centrifuge operated at 10000 rpm for 30 min. Collect and measure the total amount of the supernatant by pipetting out 1 ml, making the necessary dilution and filtering using the membrane filter, and then use a UV spectrometer to measure the percentage for the BCBA at a maximum 340 nm [14].

$$\text{Free drug (mg)} = \frac{\text{Concentration (µg/ml) X Dilution factor X Volume of supernatant}}{1000}$$

$$\%\,\text{Entrapment efficiency (\% EE)} = \frac{\text{Total amount of drug (mg) - Free drug (mg)}}{\text{Total amount of drug (mg)}} \text{X } 100$$

In vitro drug release

To investigate the rates of release of BCBA from the corresponding nanoparticle system, an *in vitro* drug release analysis was carried out. The dialysis membrane (molecular weight cut-off of the membrane was around 12000-14000 Da (pore diameter); Himedia, Mumbai) is used for the evaluation in the dialysis bag method. The pores on the dialysis membrane were opened by soaking it in normal saline over night. 500 mg equivalent weight of BCBA-sealed nanoparticles was positioned in the dialysis membrane [15].

At every interval, 1 ml of aliquot was pipetted out through a sample collector to measure the drug that had diffused through the dialysis membrane and replace it with a fresh buffer to maintain a constant volume of the dissolution medium. With the aid of a volumetric flask, the pipette-out sample was diluted to 10 ml, and the amount of BCBA was measured at 340 nm.

$$\text{Amount of drug released (mg)} = \frac{\text{Concentration (µg/ml) X dilution factor X volume of medium}}{1000}$$

$$\%\,\text{Drug release (\% DR)} = \frac{\text{Amount of drug release (mg)}}{\text{Total amount of drug (mg)}} \text{ X } 100$$

Release kinetics

By fitting the *in vitro* drug release data to various kinetics models, particularly the zero-order, first-order, Higuchi, Hixson Crowell, and Korsemeyer-Peppas models, and the drug release path from the formulation was determined [16, 17].

Optimization

Numerical optimization using a desirability index pretty much identical to value 1 has been used to choose the appropriate set of variables to produce the optimum outcome. The priorities set for optimization include maximizing entrapment efficiency and drug release. In addition, a comparison of the mean experimental outcomes with the predicted values and a percent error were determined to verify the optimization process. The experiment was replicated in triplicate to establish the durability of optimized conditions [18].

Release kinetics

By fitting the *in vitro* drug release data to different kinetics models, particularly the zero order, first order, Higuchi, Hixson Crowell, and Korsmeyer-Peppas models, the release mechanism of the drug from the optimized formulation is analyzed.

Characterization of optimized nanoparticles

Fourier transform infrared (FTIR) studies

Spectral FTIR studies were analyzed using the pressed pellet method. In this procedure, potassium bromide and a sample were collected in a 1:100 ratio. The combination formed a thin, translucent compressed disc when it was placed in a hydraulic press with an 800 mPa vacuum pressure. Using the FTIR spectro-

photometer, scans in the 4000-400 cm-1 region were performed to establish the chemical environment of the materials.

In the study, samples of BCBA, chitosan, NaTPP, and optimized formulations were examined. To identify interactions, the resulting IR spectrum of the optimized formulation was compared with the FTIR spectrum of the pure extract and excipients [19].

X-ray diffraction (XRD) studies

Using an Xpert-proanalytical diffractometer (Shimadzu-6005), the powder X-ray diffraction patterns of BCBA, chitosan, blank nanoparticles, and optimized nanoparticles were unveiled. The samples were subjected to Cu-K radiation over a 2θ range from 0 °C to 80 °C at 56 kV and 182 Ma.

Particle size measurement

The Dynamic Light Scattering (DLS) method was used to analyze the size of optimized nanoparticles. Samples were put in square glass cuvettes after being diluted with additional water, and the movement of charged colloidal particles caused by an applied electric field was observed.

Zeta potential measurement

Using the Dynamic Light Scattering (DLS) method, the zeta potential of optimized nanoparticles was determined using a Nanopartica (HORIBA, SZ-100) compact scattering instrument. Results were documented after samples were placed in transparent disposable zeta cells.

Scanning electron microscopy (SEM)

Under a scanning electron microscope (HR-SEM) Hitachi's SU6600 at magnifications varying from 10X to 600,000X operated at an accelerating voltage of 30 kV, the structural morphological features of the optimized nanoparticle formulation were observed.

Transmission electron microscopy (TEM)

Transmission electron microscopy [JEOL (JEM-1010)] with an accelerating voltage of 80 kV was employed to investigate the surface morphology and size of the nanoparticles. Before being loaded onto a specimen container, a drop of aqueous optimized nanoparticles on the carbon-coated copper TEM grid was dried under vacuum in desiccators. Image J 1.45s software was used to assess the surface morphology and particle size of nanoparticles [20].

Stability studies

According to International Council for Harmonisation (ICH) guidelines, the longevity of optimized nanoparticles was evaluated for 15, 30, 60, and 90 d at 25 °C and 60% relative humidity (RH), 450 °C and 65% RH, and 600 °C and 75% RH. After 15, 30, 60, and 90 d, the optimized nanoparticles' morphological characteristics and *in vitro* drug release were investigated.

RESULTS AND DISCUSSION

UV spectral analysis of BCBA

BCBA solution was scanned in the range of 200 to 400 nm. The absorption maximum was found to be 340 nm used for further studies as shown in fig. 1.

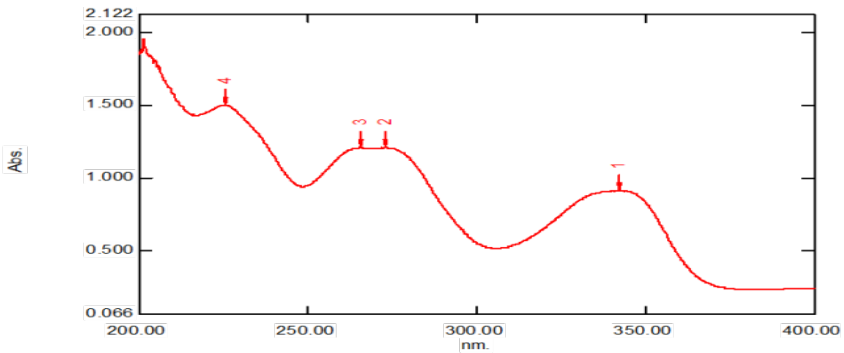

Fig. 1: UV-Vis absorption spectra of BCBA

Box behnken experimental design (BBD)

Using Design Expert version 11, BBD was used to optimize BCBANPs. In accordance with BBD, 17 formulation runs with five center points were generated using low, medium, and high levels of formulation factors in order to measure the design accuracy shown in table 2. The analysis of variance (ANOVA) factorial was additionally applied to evaluate the statistical model's authenticity.

Table 2: Independent variables, levels, and range used in BBD for BCBANPs

Levels						
Independent variables	**Low**		**Middle**		**High**	
	Coded	**Actual**	**Coded**	**Actual**	**Coded**	**Actual**
A: Amount of Polymer	-1	1.25	0	1.5	+1	1.75
B: Amount of Crosslinker	-1	0.75	0	1	+1	1.25
C: Amount of Drug	-1	400	0	450	+1	500

Polymer: chitosan (g), Cross linker: NaTPP (g), Drug: BCBA (mg)

For the preparation of BCBANPs, the above formulation table 2 listed the coded and actual independent factors (amount of polymer, cross-linker, and drug) with desired responses, including % EE (R1) and % DR (R2).

In the current study, the optimization was established using a BBD with three factors and three levels. Chitosan, NaTPP, and BCBA are the three variables that were selected. %EE and %DR are the two dependent variables specified for the research. Trials at various extreme levels were conducted in order to establish the levels of high, middle, and low for each factor. Depending on the results of the trails, the low (-1), middle (0), and high (+1) levels for BCBANPs are 1.25g, 1.5g, and 1.75g for chitosan, 0.75g, 1g, and 1.25g for NaTPP, and 400 mg, 450 mg, and 500 mg for BCBA displayed in table 2.

By inputting the data regarding the levels of factors, design expert software version 11 is employed to generate the required experimental runs. With five centre points in BCBANPs, the design expert program version 11 generates a total of 17 trial runs. At the central point, all variables are in the middle.

Table 3: Amount of each independent variable and observed responses of 17 formulations of BCBA

Factors				Responses[a]	
Runs	**A**	**B**	**C**	**R1 (%)**	**R2 (%)**
1	1.25	1	400	81.25±0.66	71.6±2.27
2	1.5	0.75	500	80±0.23	83.5±2.91
3	1.5	1	450	85.64±0.73	80.7±3.21
4	1.75	1	500	82.6±0.44	86.3±2.76
5	1.5	1	450	85.87±0.67	79.8±2.38
6	1.75	1	400	829±0.62	80.6±2.91
7	1.75	0.75	450	87.03±0.92	82.2±2.63
8	1.5	1	450	85.41±0.73	80.5±2.62
9	1.5	1	450	85.18±0.47	81.5±2.97
10	1.75	1.25	450	88.42±1.62	89.5±2.68
11	1.25	0.75	450	82.4±0.37	70.6±2.63
12	1.5	1.25	500	81.45±0.82	87.3±2.97
13	1.5	1.25	400	84.11±0.78	81.5±1.86
14	1.25	1	500	80.2±0.54	85.6±2.46
15	1.25	1.25	450	84.02±1.23	85.2±2.46
16	1.5	0.75	400	82.55±0.27	67.5±2.67
17	1.5	1	450	84.95±0.74	84±2.07

A: Amount of Chitosan (g), B: Amount of NaTPP (g), C: BCBA (mg), R1: % EE, R2: % DR. Results mentioned are mean±SD; n=3.

Polynomial equation for BCBANPs

The quality characteristics of BCBANPs were assessed by BBD through a polynomial equation in relation to response R1 (% EE) and R2 (% DR) independent variables. The values of factors were substituted in equation (1) to obtain the actual values of the response as:

% EE = 85.41+1.95 A+0.7525 B-1.13 C-0.0575 AB-0.4350 AC-0.0275 BC+0.1950 A2-0.1375 B2-3.24 C2.

% DR = 81.30+3.20 A+4.96 B+5.19 C-1.83 AB–2.08 AC-2.55 BC+0.83 A2–0.25 B2–1.10 C2.

Fitting of data in the selected model

The quadratic model was reported to be the best-fit model for both % EE and % DR after fitting the data of the observed dependent variables into distinct models. The positive and negative signs in the polynomial regression equations indicate synergistic and antagonistic effects, respectively.

Effect of variables on responses

The independent variables A (chitosan), B (NaTPP), and C (BCBA) significantly affected the responses % EE (R1) and % DR (R2) shown in table 4. The synergistic or antagonistic nature of the relationship between the variables, as well as its endurance, is shown by the sign and magnitude of the regression coefficient. For % EE, the regression coefficient of variables A and B shows a positive sign, while C is a negative sign, whereas % DR shows a positive sign for all variables. According to the regression coefficient, chitosan had a significant impact on the % EE, whereas NaTPP and BCBA had a significant influence on the % DR.

Table 4: Regression coefficients of Actual values and model adequacies for responses of BCBA

	Responses	
	R1	**R2**
A	+1.95	+3.20
P value	<0.0001*	0.0008*
B	+0.7525	+4.96
P value	0.0027*	<0.0001*
C	-1.13	+5.19
P value	0.0002*	<0.0001*
AB	-0.0575	-1.83
P value	0.8133	0.0572
AC	-0.4350	-2.08
P value	0.1059	0.0362*
BC	-0.0275	-2.55
P value	0.9099	0.0156*
A^2	+0.195	+0.83
P value	0.4216	0.3266
B^2	-0.1375	-0.25
P value	0.5663	0.7586
C^2	-3.24	-1.10
P value	<0.0001*	0.2025
lack of fit F value	2.54	0.9398
lack of fit p value	0.1943	0.5003
Model F value	45.79	24.09
Model p value	<0.0001	0.0002
Residual R square	0.9833	0.9687
Adjusted R square	0.9618	0.9285
Pred R-Squared	0.8157	0.7644
C. V. %	0.5587	1.98

*Represents a significant effect on responses. R1: Percent Entrapment Efficiency, R2: Percent Drug Release

Interaction effects of variables on responses

The interaction effects of the factors had no statistically significant effect on the % EE, while the AC (chitosan and BCBA) and BC (NaTPP and BCBA) had an impact on the % DR shown in table 4. The negative sign, which denotes negative impacts on % DR, is seen in both AC and BC. According to antagonistic effects, when the concentration of the two variables rises, the anticipated response diminishes, and vice versa.

Quadratic effects of variables on responses

Variable quadratic effects suggest that the square root of the variables has a major impact on the responses. Apart from the quadratic variable C^2 for the % EE, none of the other quadratic variables had a statistically significant impact on either of the responses shown in table 4. When the concentration of BCBA increases, the % EE substantially decreases, which explains why there is a rise in the free drug concentration in the nanoparticle suspension. The negative sign of the regression coefficient value of C^2 depicts an antagonistic effect on the % EE. C^2 has a very high regression coefficient value, which indicates that it has a significant impact on the % EE [21].

The residual r^2 values of 0.9833 for % EE and 0.9687 for % DR, the lack of significance of the lack of fit, and the appropriate disparity between the adjusted and predicted r^2 values certified the model-perfect fit of BCBANPs experimental data. The precision and accuracy of the model calibrated in the research design were effectively inferred from the percent coefficient of variance (% CV) of the response values used in the design.

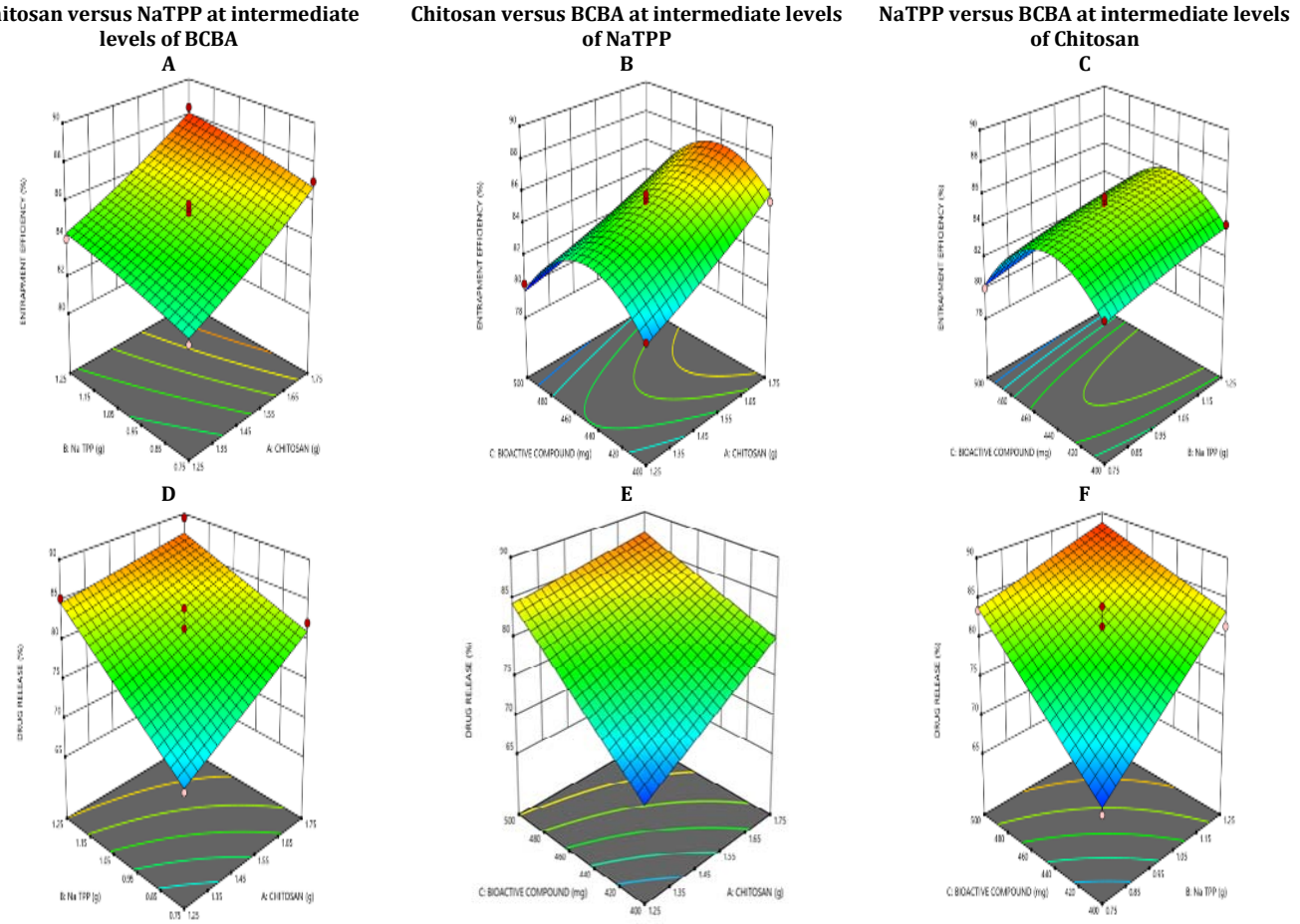

Fig. 2: (A-F): 3D Response surface plots of BCBA, R1: A-C, R2: D-F at different levels of A, B and C

Using three-dimensional surface response graphs, the impact of each independent variable on the responses of formulations with BCBANPs was further explored (fig. 2 A-F).

The effects of each independent variable on the % EE were examined in detail by the three-dimensional response graphs in fig. 2A–C. Increases in % EE were attributed to greater concentrations of A (chitosan) and B (NaTPP), as seen in fig. 2A. The gelation process is accelerated by the increasing concentration of chitosan and NaTPP, and the enhanced yield of nanoparticles further leads to the exponential growth in the % EE. Fig. 2B clearly implies that enhanced % EE occurs at high concentrations of A (chitosan) and moderate concentrations of C (BCBA). It states that while BCBA concentration tends to increase, its free drug concentration increases as well, which illustrates how BCBA's influence on % EE is affected. An enhancement in % EE was shown in fig. 2C with increased B (NaTPP) and mild C (BCBA) concentrations. The three-dimensional surface response graphs in fig. 2A, B, and C showed that the increasing concentrations of chitosan, NaTPP, and mild BCBA had a significant impact on the % EE.

The effects of each independent variable on the % DR were examined in the three-dimensional response graphs in fig. 2D-F. Fig. 2D shows how an increase in the % DR was attributed to a rise in the concentration of chitosan and NaTPP. The increasing concentration of A (chitosan) and C (BCBA) attributable to the rise in the % DR, according to 3D plot 2E, was indicated. According to the concentration gradient hypothesis, an increase in the amount of BCBA incorporated in nanoparticles correlates to a cumulative increase in drug delivery, according to fig. 2F, an increase in B (NaTPP) and C (BCBA) concentrations results in an increase in the % DR. Consequently, to maximize the % DR, a higher concentration of A (chitosan), B (NaTPP), and C (BCBA) was needed in the optimization phase [22].

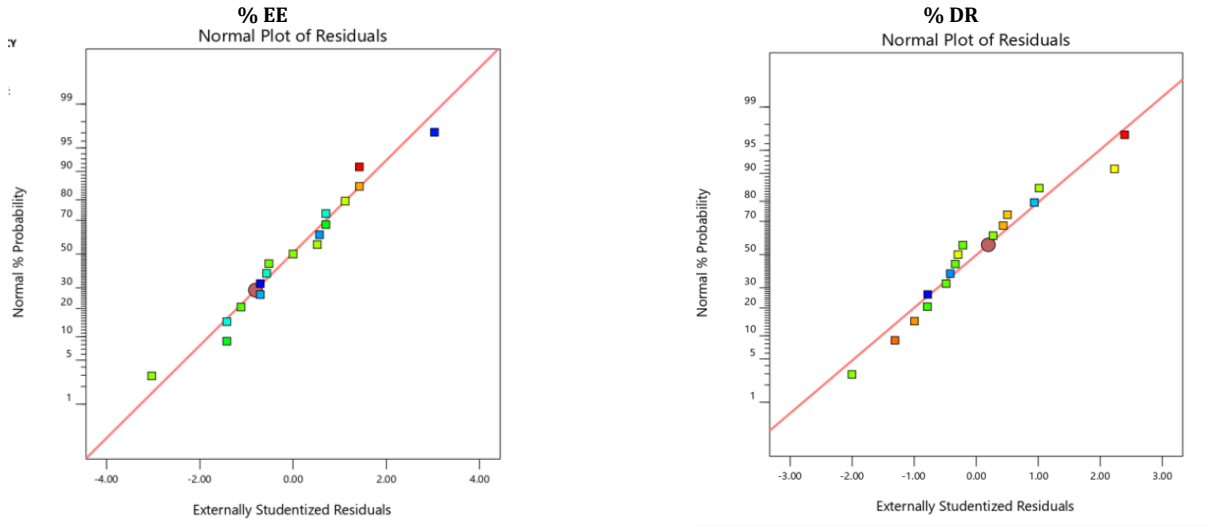

Fig. 3: Externally studentized/shalfway plots of responses of BCBANPs, R1 and R2

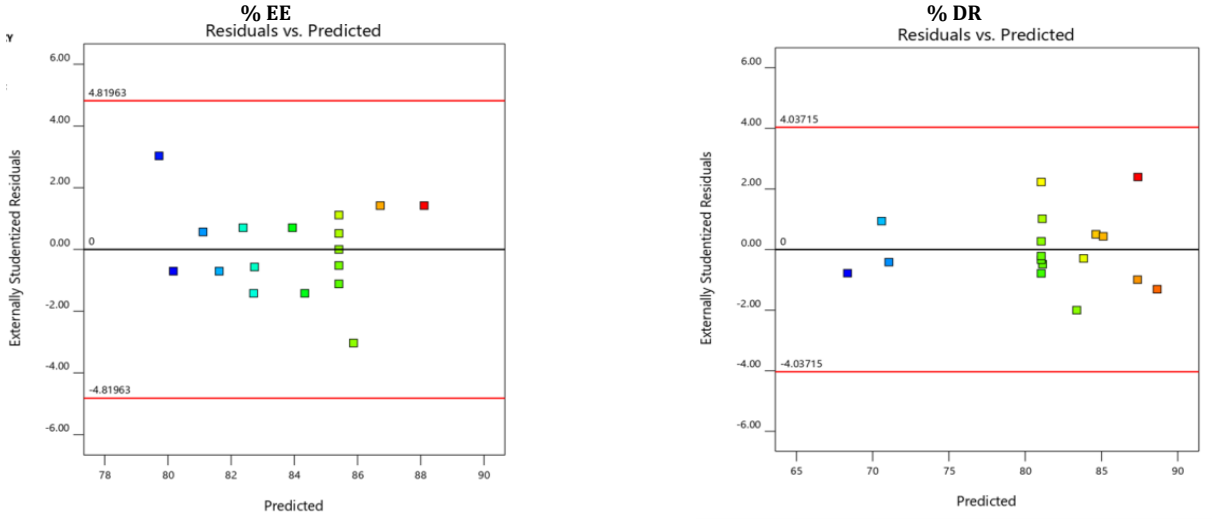

Fig. 4: Residual vs predicted plots of responses of BCBANPs, R1 and R2

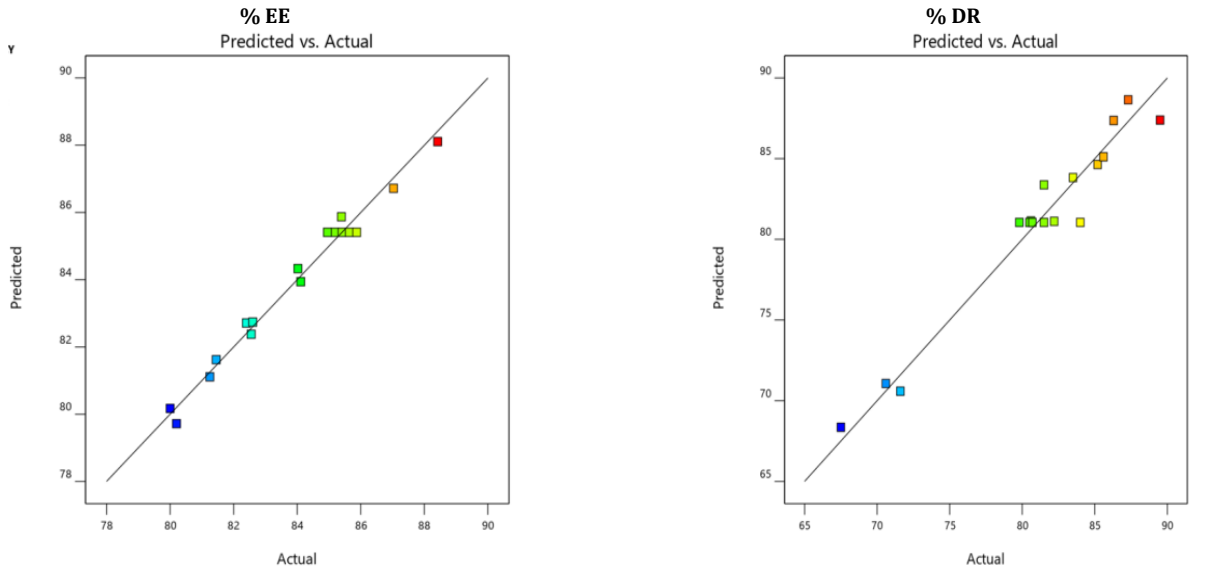

Fig. 5: Predicted vs actual plots of responses of BCBANPs, R1 and R2

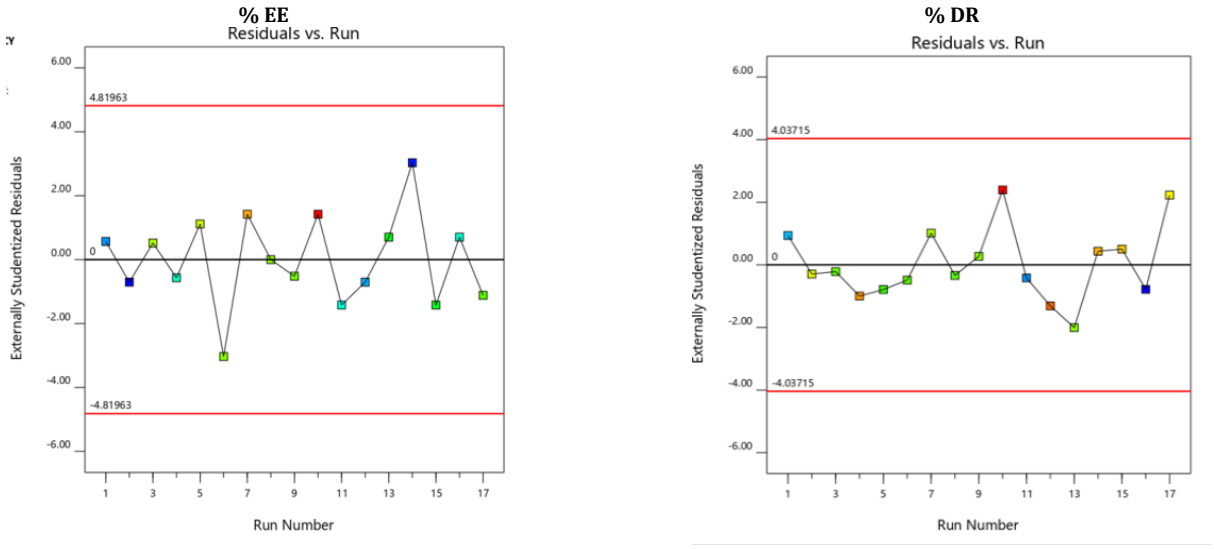

Fig. 6: Residual vs Run plots of responses of BCBANPs, R1 and R2

Chitosan versus NaTPP at intermediate levels of BCBA

Chitosan versus BCBA at intermediate levels of NaTPP

NaTPP versus BCBA at intermediate levels of Chitosan

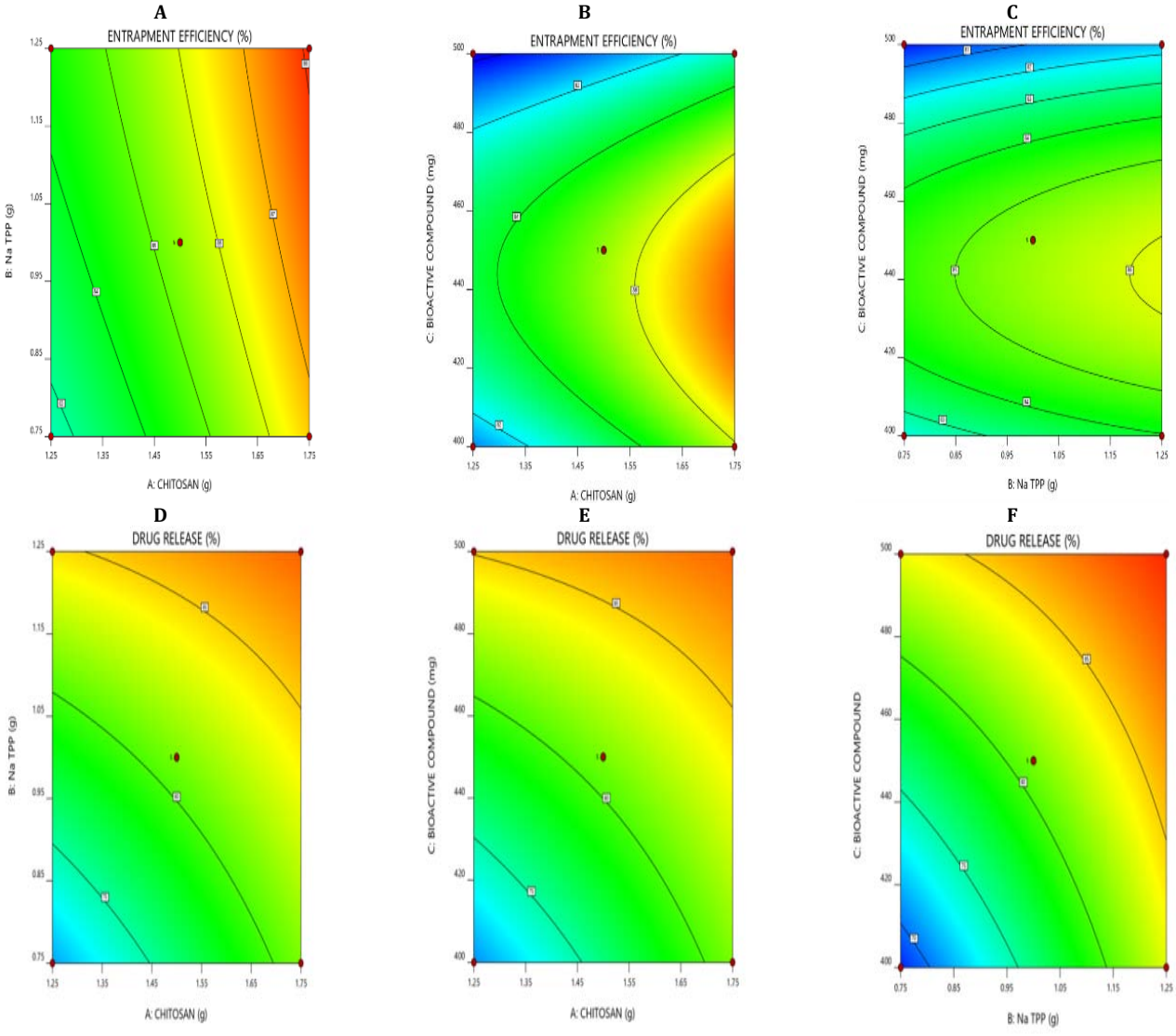

Fig. 7: 2-D plots of responses of BCBANPs, R1 and R2

Graphs imply the assessment of two factors or combination factors at a time.

Model validity plots for BCBANPs were also investigated. In fig. 3, halfway normal plots of BCBANPs were used to demonstrate that the model is significant if all residual values are nearby or lie on a straight line representing the S-shaped curve.

Fig. 4 shows the Residual vs. Expected BCBANPs responses. Data points were seen to be randomly dispersed over the boundaries (red line) to act as a megaphone sequence. It suggested that there were no outliers and demonstrated the suitability of the selected mathematical analysis for the experimental design [23].

Fig. 5 of the BCBANPs expected vs. actual plots demonstrated how closely related the predicted and experimental responses were, and they made an attempt to explain how the derived model might take into account a linear relationship between the formulation factors and responses.

Plots of the BCBANPs Responses: Residual versus Run fig. 6 makes it evident that random points were found inside the red lines and that the model that was developed was linearly correlated to the variables and responses [24].

Fig. 7 two-dimensional contour plots suggested that two variables or a combination of variables were being measured at once. Darker areas, in comparison, showed a greater proportion of specific responses were impacting them [25].

Percent entrapment efficiency (% EE)

The % EE for 17 experimental runs was found to be in the range of 80±0.23% (R2) to 88.42±1.62% (R10) portrayed in fig. 8.

***In vitro* dissolution studies of BCBANPs**

Dissolution study of BCBA loaded chitosan nanoparticles were carried with dialysis bag method as mentioned in fig. 9 to 12.

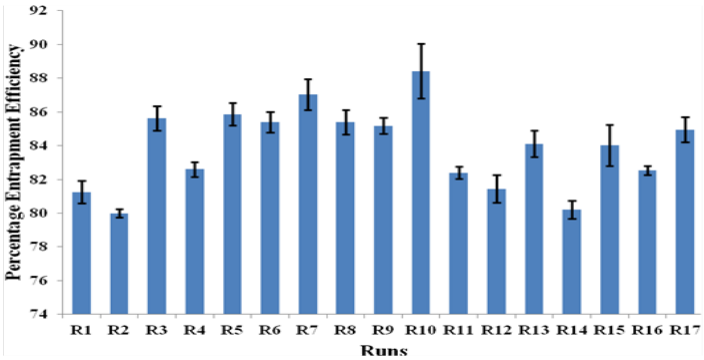

Fig. 8: % EE of BACBA runs, results mentioned are mean±SD; n=3

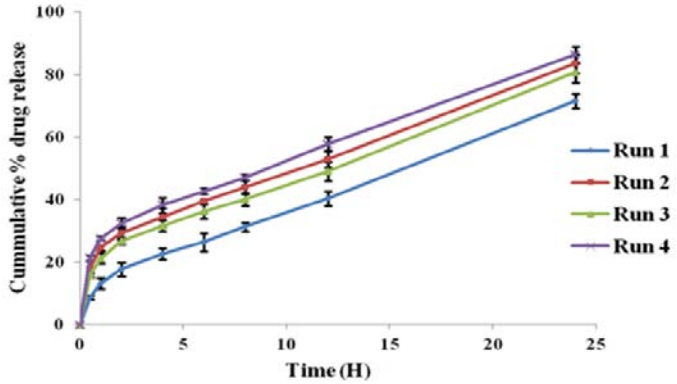

Fig. 9: *In vitro* dissolution profiles of runs 1-4 formulations of BCBANPs, results mentioned are mean±SD; n=3

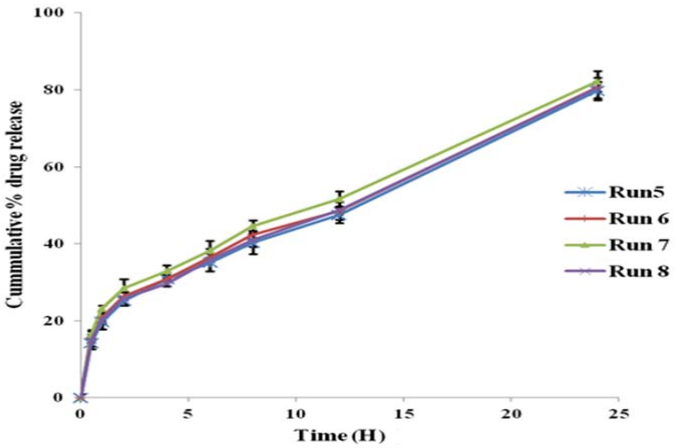

Fig. 10: *In vitro* dissolution profiles of runs 5-8 formulations of BCBANPs, results mentioned are mean±SD; n=3

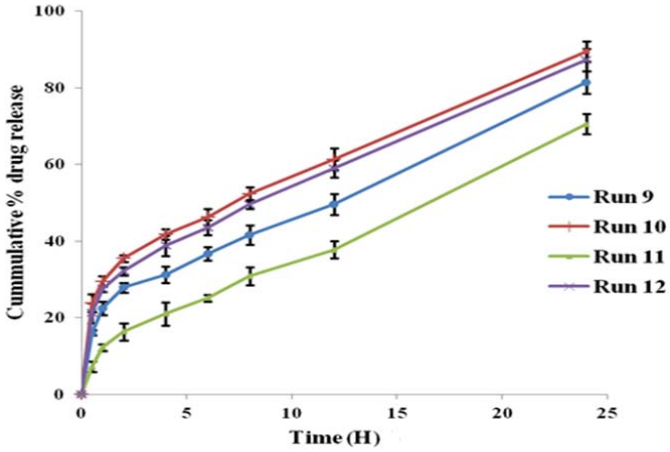

Fig. 11: *In vitro* dissolution profiles of runs 9-12 formulations of BCBANPs, results mentioned are mean±SD; n=3

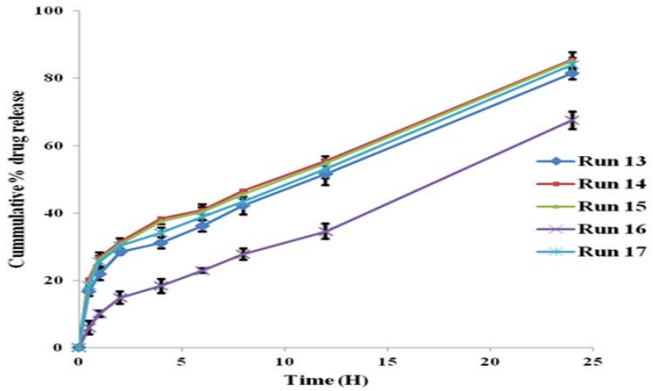

Fig. 12: *In vitro* dissolution profiles of runs 13-17 formulations of BCBANPs, Results mentioned are mean±SD; n=3

Using an *in vitro* dialysis bag mechanism with phosphate buffer saline (PBS) pH 7.4 as the dissolution medium for 24 h, the drug release performance of BCBA encapsulated in chitosan nanoparticles is investigated. According to the results at different time intervals, the drug was released from the formulation in two phases: a brief initial burst, followed by a prolonged release. All 17 formulations had first bursts at 30 min that ranged from 5.9% to 23.9%, according to R16 and R10 formulations, respectively. The cumulative amount of drug released from nanoparticles over the course of 24 h ranges from 67.5% to 89.5%. In fig. 9 to 12, the R16 and R10 formulations showed the lowest and maximum drug release, with 67.5% and 89.5%, respectively.

The disparity in formulations entrapment efficiency may be the cause of the drug inconsistent release. The amount of drug trapped in nanoparticles is strongly correlated with the amount of drug release, according to earlier research. In comparison to formulations with poor entrapment efficiency, those with high entrapment efficiency have the maximal release of the drug at the relevant intervals and enhance the diffusion rate as a result of an early upswing in the concentration gradient. This might illustrate why the R10 formulation had the maximum entrapment efficiency of 88.42% and the lowest drug release was seen in the R16 formulation, which had an entrapment efficiency of 82.55%.

Table 5: Release kinetics of BCBANPs

Runs	Zero order (r)	First order (r)	Higuchi (r)	Hixson crowell (r)	Korsemeyer Peppas	
					(r)	(n)
R1	0.9242	0.9831	0.9786	0.9779	0.9874	0.4909
R2	0.7334	0.9699	0.9798	0.9417	0.9815	0.3574
R3	0.7982	0.9718	0.9834	0.9517	0.9826	0.3852
R4	0.6840	0.9691	0.9714	0.9338	0.9809	0.3283
R5	0.8166	0.9731	0.9861	0.9543	0.9867	0.4033
R6	0.7969	0.9716	0.9840	0.9502	0.9833	0.3848
R7	0.7596	0.9712	0.9826	0.9449	0.9828	0.3753
R8	0.8157	0.9743	0.9857	0.9560	0.9837	0.3955
R9	0.7776	0.9702	0.9808	0.9474	0.9781	0.3723
R10	0.5730	0.9719	0.9664	0.9354	0.9861	0.3194
R11	0.9418	0.9834	0.9732	0.9819	0.9875	0.5316
R12	0.6513	0.9722	0.9752	0.9401	0.9854	0.3363
R13	0.7817	0.9736	0.9828	0.9503	0.9783	0.3718
R14	0.6739	0.9683	0.9734	0.9359	0.9804	0.3364
R15	0.6946	0.9680	0.9752	0.9376	0.9808	0.3454
R16	0.9592	0.9833	0.9633	0.9857	0.9883	0.5657
R17	0.7259	0.9685	0.9754	0.9412	0.9744	0.3458

Results were mentioned as the number of experiments (n=3)

The 17 runs of BCBANPs at different time intervals yielded drug release profile data that was fitted to a variety of drug release kinetic models, including zero order, first order, higuchi, the Hixson Crowell model, and the Korsmeyer peppas. As shown in the table, the Higuchi and Korsmeyer peppas models were determined to have the highest correlation coefficient value (r). The maximal r value for the Higuchi and Korsmeyer Peppas model indicated that formulation swelling caused drug diffusion into the dissolving media. In all formulations, the n value for the Korsmeyer-Peppas model spans from 0.3194 to 0.5316, as shown in table 5. The n value of the Korsmeyer-Peppas model revealed that fickian diffusion was the mechanism responsible for drug release from the nanoparticle formulation, with the exception of the R11 formulation. In fickian diffusion, the rate of drug diffusion from the nanoparticle is inversely proportional to the thickness of the polymeric membrane and directly proportional to the surface area and concentration gradient.

Optimization of BCBANPs

Optimization of BCBA loaded chitosan nanoparticles were done by using numerical optimization technique as given in table 10.

Table 6: Predicted and experimental responses of numerical optimization BCBANPs

Factors	Predicted values	Actual operable optimal conditions	Responses	Predicted responses	Experimental responses
Chitosan	1.43 g	1.43 g	% EE	84.73 %	83.7±1.83 %
NaTPP	0.937 g	0.94 g	% DR	77.49 %	78.33±2.92%
BCBA	438.133 mg	438 mg			

Results were mentioned as mean±SD; n=3

Optimization of BCBANPs (OBCBANPs) was done by using numerical optimization techniques to maximize the percent entrapment efficiency and percent drug release.

The optimized formulation was generated with predicted values of chitosan 1.43 g, NaTPP 0.937 g, and BCBA 438.133 g and predicted responses, i.e., % EE and % DR, as 84.73% and 77.49%, respectively. The experimental responses were found to be 83.7% and 78.33% for % EE and % DR respectively mentioned in table 6.

The optimization method was further validated by comparing the experimental and predicted responses with percent errors ranging from 2.71 to 3.48%.

Table 7: Release kinetics of OBCBANPs

Run	Zero order (r)	First order (r)	Higuchi (r)	Hixson crowell (r)	Korsemeyer Peppas	
					(r)	(n)
OBCBANPs	0.843	0.9784	0.9890	0.9630	0.9891	0.4271

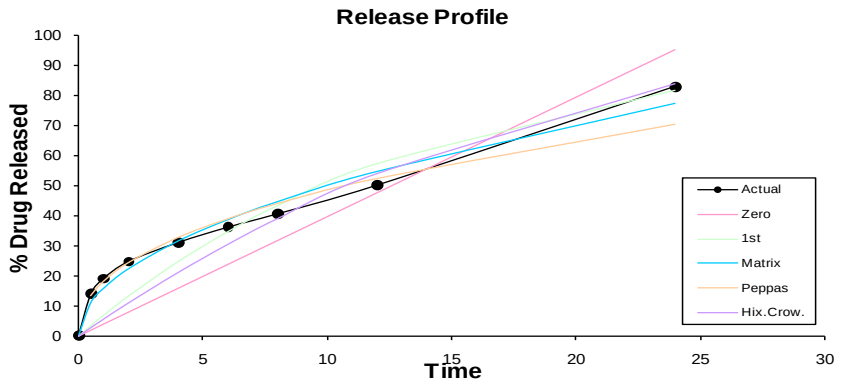

Fig. 13: Release kinetics of OBCBANPs

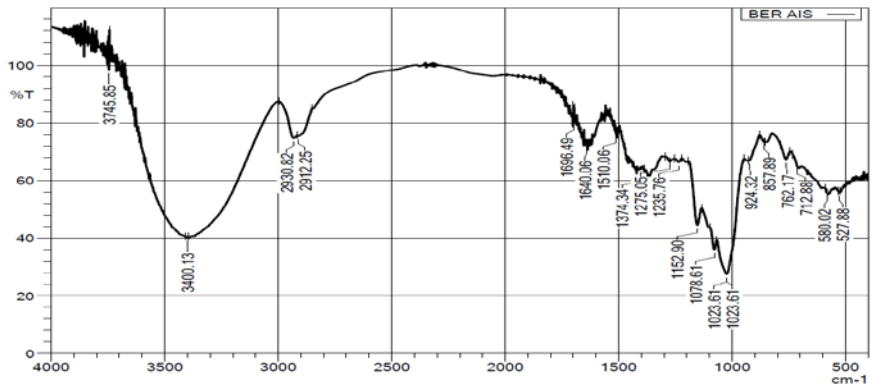

Fig. 14: FTIR spectra of BCBA

A variety of drug release kinetic models, including zero order, first order, higuchi, the Hixson-Crowell model, and the Korsmeyer Peppas model, were fitted to the drug release profile data from OBCBANPs that were recorded at various time intervals. As shown in the table, the Higuchi and Korsmeyer peppas models were found to have the highest correlation coefficient value (r). The maximal r value for the Higuchi and Korsmeyer Peppas model revealed that formulation swelling caused drug diffusion into the dissolving media. The n value for the Korsmeyer-Peppas model is 0.4271, as shown in fig. 13 and table 7, respectively. The n value of the Korsmeyer-Peppas model showed that Fickian diffusion was the mechanism responsible for drug release from the optimized formulation. In Fickian diffusion, the rate of drug diffusion from the nanoparticle is inversely related to the thickness of the polymeric membrane and directly proportional to the surface area and concentration gradient.

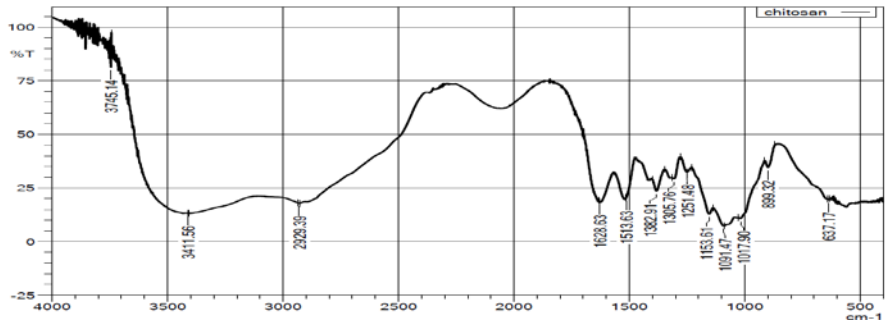

Fig. 15: FTIR spectra of chitosan

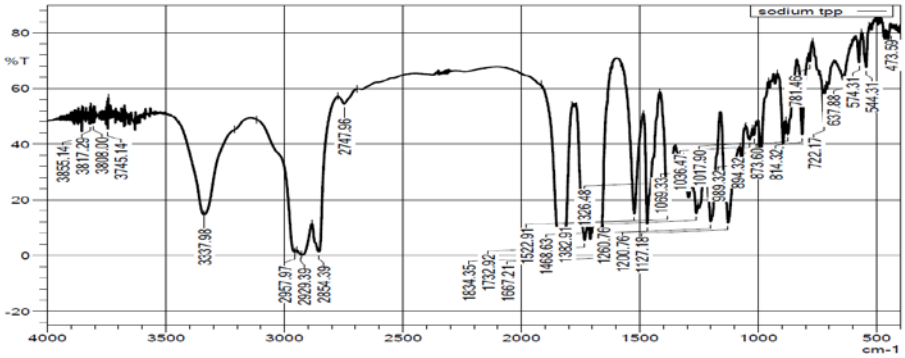

Fig. 16: FTIR spectra of NaTPP

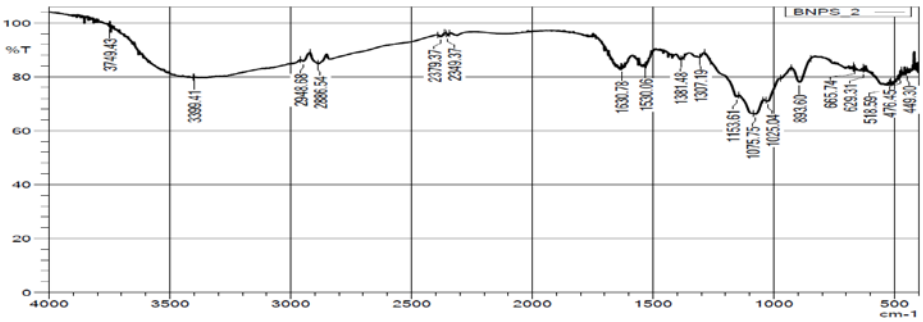

Fig. 17: FTIR spectra of OBCBANPs, The FTIR studies reported compatibility of BCBA with chitosan and NaTPP, and no significant interactions were observed (fig. 14-17)

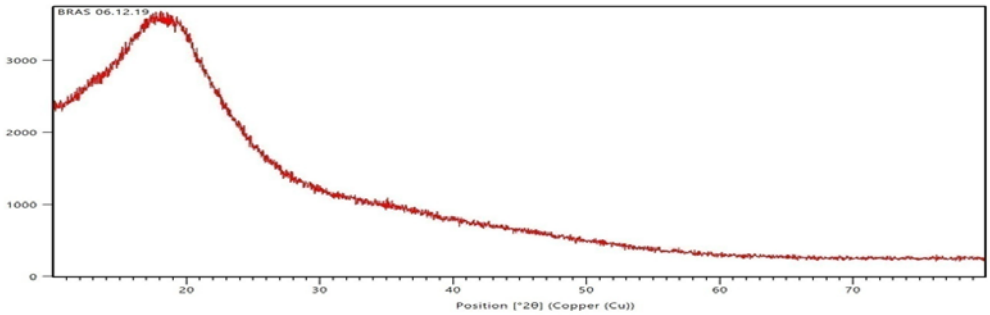

Fig. 18: XRD of BCBA, the BCBA showed no sharp peaks at 2θ scattered angles, which confirmed the amorphous nature (fig. 18)

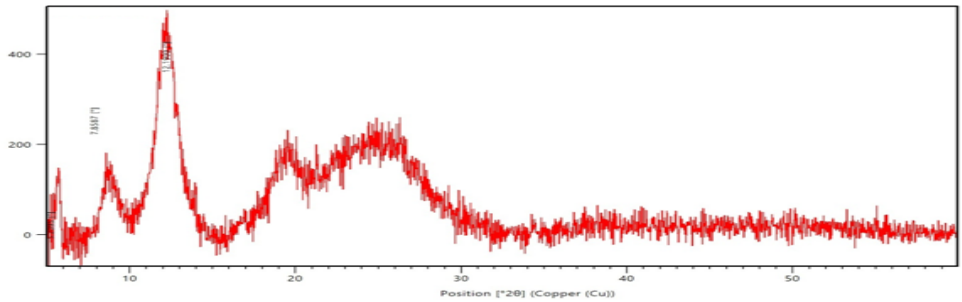

Fig. 19: XRD of chitosan, the XRD of chitosan showed a sharp peak at a 2θ scattered angle of 12.10 indicating a slightly crystalline nature (fig. 19)

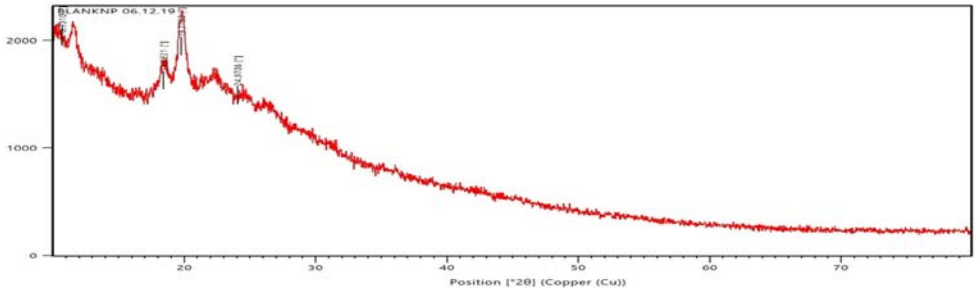

Fig. 20: XRD of blank nanoparticles, the XRD of the blank nanoparticle showed sharp peaks at 2θ scattered angles of 12.1°, 18.42°, 19.77°, and 24.07°, indicating the crystalline nature due to the gelation of chitosan and NaTPP (fig. 20)

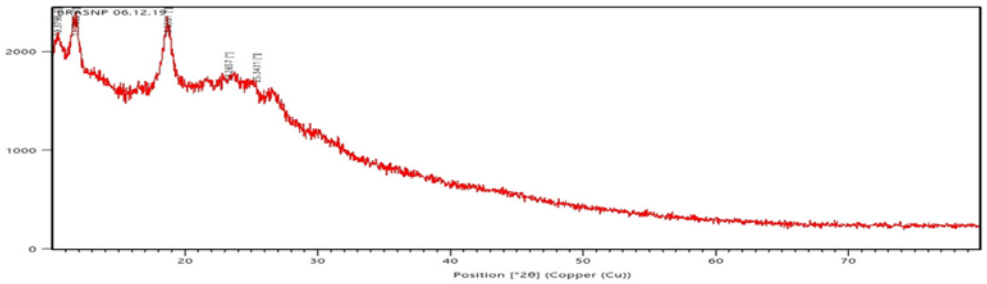

Fig. 21: XRD of OBCBANPs, the optimized formulation of OBCBANPs showed sharp peaks at 2θ scattered angles of 11.7°, 18.65°, and 23.26°, indicating that the BCBA entrapped chitosan nanoparticle exhibits a crystalline nature (fig. 21)

Particle size

Particle size measurements were required to confirm the formation of nano-range particles. The frequency (percent/nm) on the Y-axis vs diameter (nm) on the x-axis was reported in the particle size distribution spectra for optimized chitosan nanoparticles. The hydrodynamic diameter of the hydrosol was examined using the dynamic light scattering method (particle suspension).

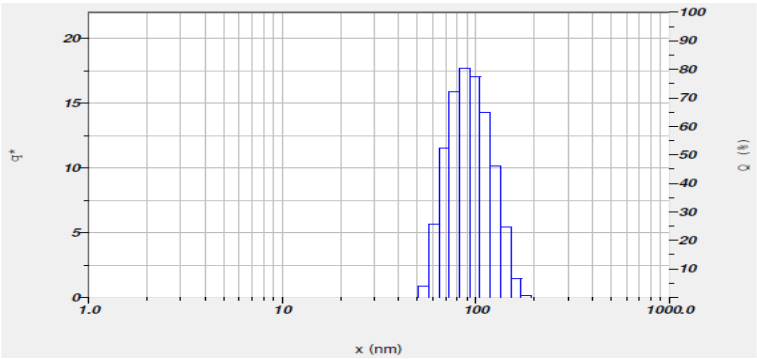

Calculation Results

Peak No.	S.P.Area Ratio	Mean	S. D.	Mode
1	1.00	95.4 nm	23.6 nm	87.9 nm
2	—	--- nm	--- nm	--- nm
3	—	--- nm	--- nm	--- nm
Total	1.00	95.4 nm	23.6 nm	87.9 nm

Fig. 22: Particle size of OBCBANPs, the OBCBANPs particle size was determined to be 95.4 nm, as shown in fig. 22. The findings demonstrated the particles' nanoscale size, which is critical in the production of nanoparticles

Zeta potential

The formulation is stabilized by the zeta potential, an electrical charge on the particle surface that acts as a repulsive force. The optimized chitosan nanoparticle zeta potential spectra were captured as zeta potential versus intensity spectra, with intensity (a. u.) on the y-axis and zeta potential (mV) on the x-axis. The DLS technique was utilized to investigate the hydrosol zeta potential (particle suspension). Strong negative or positive zeta potential hydrosols strive to reject one another, limiting the possibilities of particle aggregation. Furthermore, there won't be any pressure to prevent the particles from adhering to one another and flocculating if the zeta potential values of the particles are weak.

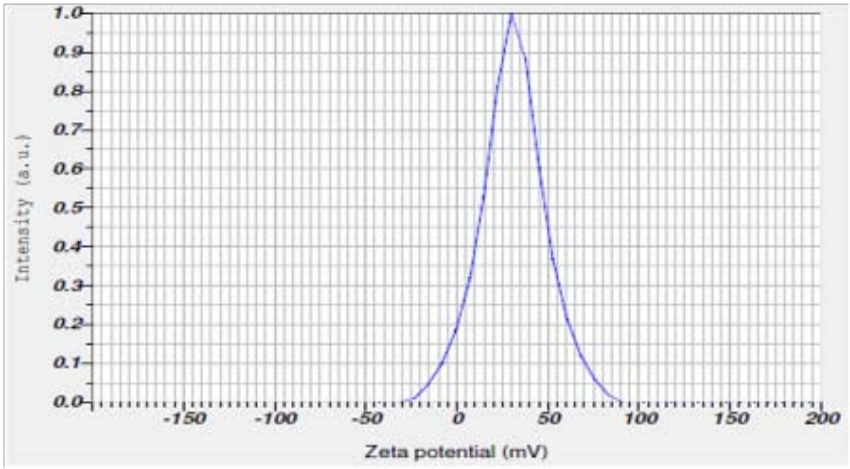

Fig. 23: Zeta potential of OBCBANPs

The zeta potential value of 31 mV was found to be positive, implying that the synthesized OBACBANPs had greater stability by inhibiting particle aggregation, as shown in fig. 23. The positive zeta potential value might be attributed to Chitosan's cationic structure and the presence of residual amino groups that are not neutralized by interactions with NaTPP molecules discussed in previous research works.[26] Such amino groups are resistant to anion adsorption and have a high electrical double layer thickness, resulting in healthy nanoparticles.

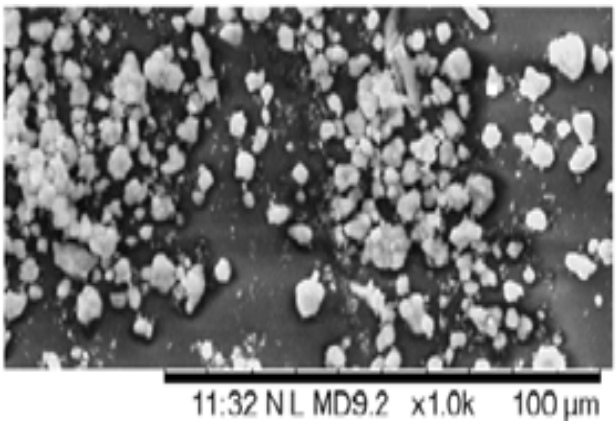

Fig. 24: SEM of OBCBANPs

Scanning electron microscopy (SEM)

The surface morphology of OBCBANPs viewed in SEM images turns out to be spherical in form with a homogeneous distribution, as shown in fig. 24. The OBCBANPS exhibited low aggregation, somewhat rough surface, and a mean diameter below 100 nm, according to SEM analysis. A sufficient zeta potential of the particle for repelling the suggested potential stabilization of the nanoparticles is directly responsible for the lowest possible aggregation proved in earlier works [27].

Transmission electron microscopy (TEM)

According to TEM images shown in fig. 25, the OBCBANPs employed in this study had a mean diameter of less than 100 nm. Formed OBCBANPs are observed to be spherical in form and tend to be partially aggregated.

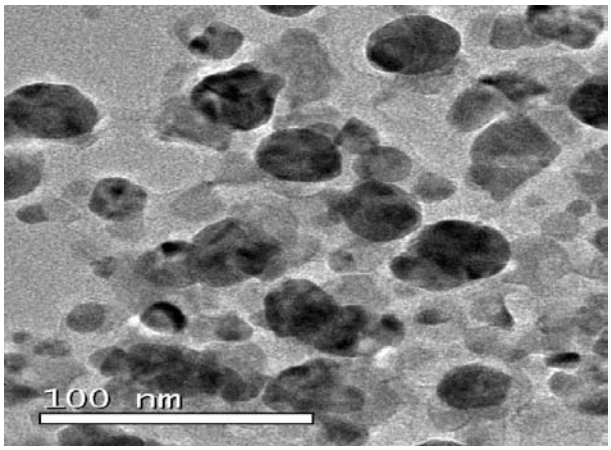

Fig. 25: TEM of OBCBANPs

Stability testing of OBCBANPs

OBCBANPs were subjected to accelerated stability testing, and the results are tabulated below.

Table 8: Physical appearance of optimized OBCBANPs during stability studies

Physical appearance of optimized OBCBANPs					
Accelerated conditions	**Formulation**	**15 d**	**30 d**	**60 d**	**90 d**
25 °C/60% RH		Intact	Intact	Intact	Intact
45 °C/65% RH	OBCBANPs	Intact	Intact	Intact	Intact
60 °C/75% RH		Intact	Intact	Intact	Intact

Results were mentioned as the number of experiments (n=3)

Table 9: % Drug release data of OBCBANPs during stability studies

Time (H)	**Formulation**	**15 d**		
		25 °C/60% RH	**45 °C/65% RH**	**60 °C/75% RH**
0.5		13.3±1.46	13.8±0.85	13.5±1.17
1		18.6±1.78	18.2±2.23	18.9±0.57
2		23.9±0.67	23.4±1.43	24.8±1.70
4	OBCBANPs	29.8±0.74	29.3±1.65	30.5±0.95
6		34.1±2.56	34.4±1.21	33.9±0.78
8		38.3±0.67	38.9±1.39	39.7±1.03
12		58.9±2.72	59.2±1.25	58.1±0.46
24		78.8±1.78	79.1±0.56	78.3±1.65
		30 d		
		25 °C/60% RH	45 °C/65% RH	60 °C/75% RH
0.5		12.8±0.74	13.2±1.48	13.9±0.93
1		18.9±1.86	18.2±0.78	19.1±2.71
2		23.2±0.92	24.3±3.01	23.6±1.83
4		29.3±0.87	30.1±1.29	29.8±2.01
6	OBCBANPs	34.8±1.56	33.8±0.76	34.3±1.93
8		38.5±0.64	38.1±3.13	39.3±1.87
12		58.6±1.68	58.3±0.79	59.2±2.69
24		79.2±0.88	78.8±1.28	78.2±0.61
		60 d		
		25 °C/60% RH	45 °C/65% RH	60 °C/75% RH
0.5		12.8±1.63	13.2±0.47	13.7±2.26
1		18.7±1.97	18.2±0.75	19.1±1.46
2		23.9±1.55	23.5±0.58	24.2±3.05
4	OBCBANPs	29.5±0.73	29.1±1.35	30.6±2.47
6		34.3±2.18	33.8±0.95	34.9±1.75
8		38.7±2.43	39.2±0.89	38.2±1.56
12		58.3±1.07	59.4±2.13	58.7±0.78
24		78.4±0.77	79.3±1.68	78.7±2.19
		90 d		
		25 °C/60% RH	45 °C/65% RH	60 °C/75% RH
0.5		12.8±2.67	13.4±0.86	12.5±1.58
1		18.7±2.18	19.3±0.76	18.6±1.37
2		23.7±0.89	23.9±1.74	24.5±2.43
4	OBCBANPs	29.8±1.68	30.4±0.87	29.1±2.09
6		33.9±1.57	34.4±0.79	33.2±1.34
8		38.4±1.46	38.9±2.63	39.4±0.67
12		58.5±0.97	59.4±1.57	58.7±2.18
24		79.8±1.28	77.5±0.54	78.3±1.76

Results mentioned are mean±SD; n=3.

The stability tests were performed in triplicate for 90 d at 25 °C/60% RH, 45 °C/65% RH and 60 °C/75% RH and assessed for appearance and percent drug release at 15, 30, 60, and 90 d, respectively. Stability tests of OBCBANPs, therefore, illustrated that there is no substantial variation in appearance and % DR spotted in Tables 12 to 13. Stability studies indicate that OBCBANPs are robust for up to 90 d.

CONCLUSION

The ionic gelation method is employed in the preparation of BCBANPs. BBD is practiced to achieve desired experimental runs for optimization to cut short the wide range of experimental runs. The regression coefficients established by the second-order polynomial equations of all the responses indicated that the model is significant. Diagnostic plots showed that the quadratic model generated was well-matched to all aspects of the experimental design. BCBANPs were optimized with the numerical optimization technique by setting the concentrations of independent variables chitosan, NaTPP, and BCBA at 1.43 g, 0.94 g and 438 mg, respectively, to get the maximum desired responses, which include % EE and % DR of 84.73% and 77.49%, respectively. FTIR studies revealed compatibility among the drug and excipients; XRD studies stated the crystalline nature of nanoparticles due to the gelation of chitosan and NaTPP. The particle size of the optimized formulation was measured to be 95.4 nm, substantiating that the nanoparticles are in the nanorange. Zeta potential recorded at 31 mV inferred the superlative stability of optimized formulation nanoparticles. SEM and TEM analyses illustrated that optimized nanoparticles are spherical in form and homogeneous with minimum aggregation. Accelerated stability studies performed on the optimized formulation stated that there was no substantial variation in appearance and % DR. The presence of glucosamine groups in chitosan serves as a ligand for the megalin receptors associated with renal tubular epithelial cells. Therefore, stable optimized nanoparticles further need to be investigated and established for antiurolithiatic activity by targeting the kidney by performing *in vivo* studies.

ACKNOWLEDGEMENT

The authors are grateful to Sri Padmavathi School of Pharmacy for providing the research facilities.

FUNDING

Nil

AUTHORS CONTRIBUTIONS

The authors of this manuscript share an equal contribution in all stages of the manuscript up to the approval of the final version.

CONFLICTS OF INTERESTS

Declared none

REFERENCES

1. Kumari A, Yadav SK, Yadav SC. Biodegradable polymeric nanoparticles based drug delivery systems. Colloids Surf B Biointerfaces. 2010;75(1):1-18. doi: 10.1016/j.colsurfb.2009.09.001, PMID 19782542.
2. Tønnesen HH, Karlsen J. Alginate in drug delivery systems. Drug Dev Ind Pharm. 2002;28(6):621-30. doi: 10.1081/ddc-120003853, PMID 12149954.
3. Asgharian S, Lorigooini Z, Rafieian R, Rafieian Kopaei M, Kheiri S, Nasri H. The preventive effect of Berberis vulgaris extract on contrast-induced acute kidney injury. J Nephropathol. 2017;6(4):395-8. doi: 10.15171/jnp.2017.65.
4. Balaji LG, Banji D, Banji JF. Evaluation of antiurolithiatic activity of the aqueous and alcoholic extracts of roots of *boerhaavia diffusa*. Indo Am J Pharm Res. 2015;5(1):525-30. doi: 10.1044/1980-iajpr.150115.
5. Geng X, Zhang M, Lai X, Tan L, Liu J, Yu M. Small-sized cationic miRi-PCNPs selectively target the kidneys for high-efficiency antifibrosis treatment. Adv Healthc Mater. 2018;7(21):e1800558. doi: 10.1002/adhm.201800558, PMID 30277665.
6. Wang J, Masehi Lano JJ, Chung EJ. Peptide and antibody ligands for renal targeting: nanomedicine strategies for kidney disease. Biomater Sci. 2017;5(8):1450-9. doi: 10.1039/c7bm00271h, PMID 28516997.
7. Gao S, Hein S, Dagnæs Hansen F, Weyer K, Yang C, Nielsen R. Megalin-mediated specific uptake of chitosan/siRNA nanoparticles in mouse kidney proximal tubule epithelial cells enables AQP1 gene silencing. Theranostics. 2014;4(10):1039-51. doi: 10.7150/thno.7866, PMID 25157280.
8. Qiao H, Sun M, Su Z, Xie Y, Chen M, Zong L. Kidney-specific drug delivery system for renal fibrosis based on coordination-driven assembly of catechol-derived chitosan. Biomaterials. 2014;35(25):7157-71. doi: 10.1016/j.biomaterials.2014.04.106.
9. El-ASSAL MI, Samuel D. Optimization of rivastigmine chitosan nanoparticles for neurodegenerative alzheimer; *in vitro* and ex vivo characterizations. Int J Pharm Pharm Sci. 2022;14(1):17-27. doi: 10.22159/ijpps.2022v14i1.43145.
10. Yuan ZX, Zhang ZR, Zhu D, Sun X, Gong T, Liu J. Specific renal uptake of randomly 50% N-acetylated low molecular weight chitosan. Mol Pharm. 2009;6(1):305-14. doi: 10.1021/mp800078a, PMID 19035784.
11. Patel M, Patel NV, Patel TB. Design and development of rilpivirine nanoparticle containing chitosan using ionic gelation method for hiv infections. Int J Pharm Pharm Sci. 2020;12(2):113-8. doi: 10.22159/ijpps.2020v12i2.35814.
12. Vozza G, Danish M, Byrne HJ, Frias JM, Ryan SM. Application of box-behnken experimental design for the formulation and optimisation of selenomethionine-loaded chitosan nanoparticles coated with zein for oral delivery. Int J Pharm. 2018;551(1-2):257-69. doi: 10.1016/j.ijpharm.2018.08.050, PMID 30153488.
13. Ghose D, Patra CN, Swain S, Sruti J. Box-Behnken design-based development and characterization of polymeric freeze-dried nanoparticles of isradipine for improved oral bioavailability. Int J App Pharm. 2023;15(4):60-70. doi: 10.22159/ijap.2023v15i4.47728.
14. Mao CF, Zhang XR, Johnson A, He JL, Kong ZL. Modulation of diabetes mellitus-induced male rat reproductive dysfunction with micro-nanoencapsulated echinacea purpurea ethanol extract. BioMed Res Int. 2018;2018:4237354. doi: 10.1155/2018/4237354, PMID 30246020.
15. Abo-Elseoud WS, Hassan ML, Sabaa MW, Basha M, Hassan EA, Fadel SM. Chitosan nanoparticles/cellulose nanocrystals nanocomposites as a carrier system for the controlled release of repaglinide. Int J Biol Macromol. 2018;111:604-13. doi: 10.1016/j.ijbiomac.2018.01.044, PMID 29325745.
16. Padmaa PM, Preethy AJ, Setty CM, Peter GCV. Release kinetics–concepts and applications. IJPRT. 2018;8(1):12-20.
17. Fu Y, Kao WJ. Drug release kinetics and transport mechanisms of non-degradable and degradable polymeric delivery systems. Expert Opin Drug Deliv. 2010;7(4):429-44. doi: 10.1517/17425241003602259, PMID 20331353.
18. Ruhi R, Sarika W, Vinay S, Ram G. Pramipexole dihydrochloride loaded chitosan nanoparticles for nose to brain delivery: development, characterization and *in vivo* anti-Parkinson activity. Int J Biol Macromol. 2018;1(109):27-35. doi: 10.1016/j. ijbiomac.2017.12.056.
19. Sonali BS, Bharate SB, Bajaj AN. Interactions and incompatibilities of pharmaceutical excipients with active pharmaceutical ingredients, a comprehensive review. J Excipients Food Chem. 2010;1(3):3-25.
20. Sharma R, Yasir M, Bhaskar S, Asif M. Formulation and evaluation of paclitaxel loaded PSA-PEG nanoparticles. J Appl Pharm Sci. 2011;1(5):96-8.
21. Gannu R, Palem CR, Yamsani SK, Yamsani VV, Yamsani MR. Enhanced bioavailability of buspirone from reservoir-based transdermal therapeutic system, optimization of formulation employing box–behnken statistical design. AAPS PharmSciTech. 2010;11(2):976-85. doi: 10.1208/s12249-010-9451-7, PMID 20517714.
22. Abul Kalam M, Khan AA, Khan S, Almalik A, Alshamsan A. Optimizing indomethacin-loaded chitosan nanoparticle size, encapsulation, and release using Box-Behnken experimental design. Int J Biol Macromol. 2016;87:329-40. doi: 10.1016/j.ijbiomac.2016.02.033, PMID 26893052.
23. Meng J, Sturgis TF, Youan BB. Engineering tenofovir-loaded chitosan nanoparticles to maximize microbicide mucoadhesion. Eur J Pharm Sci. 2011;44(1-2):57-67. doi: 10.1016/j.ejps.2011.06.007, PMID 21704704.
24. Solanki AB, Parikh JR, Parikh RH. Formulation and optimization of piroxicam proniosomes by 3-factor, 3-level box-Behnken design. AAPS PharmSciTech. 2007;8(4):E86. doi: 10.1208/pt0804086, PMID 18181547.
25. Gannu R, Palem CR, Yamsani SK, Yamsani VV, Yamsani MR. Enhanced bioavailability of buspirone from the reservoir-based transdermal therapeutic system, optimization of formulation employing box–behnken statistical design. AAPS PharmSciTech. 2010;11(2):976-85. doi: 10.1208/s12249-010-9451-7, PMID 20517714.
26. Raj R, Wairkar S, Sridhar V, Gaud R. Pramipexole dihydrochloride loaded chitosan nanoparticles for nose to brain delivery: development, characterization and *in vivo* antiparkinson activity. Int J Biol Macromol. 2018;109:27-35. doi: 10.1016/j.ijbiomac.2017.12.056, PMID 29247729.
27. Rukmangathen R, Yallamalli IM, Yalavarthi PR. Formulation and biopharmaceutical evaluation of risperidone-loaded chitosan nanoparticles for intranasal delivery. Drug Dev Ind Pharm. 2019;45(8):1342-50. doi: 10.1080/03639045.2019.1619759, PMID 31094571.